# Development and Characterisation of Completely Degradable Composite Tissue Engineering Scaffolds

PhD Thesis by Montse Charles-Harris Ferrer

PhD Supervisor: Josep A. Planell i Estany

Barcelona, July 2007

# Chapter 2: Development and optimisation of biodegradable composite scaffolds via Solvent Casting

## *Introduction*

The principles of tissue engineering and the cells, signals and scaffolds that compose it have been described in detail in the Introduction (Chapter 1). Scaffolds must fulfil a series of structural and chemical requirements in order to be suitable for tissue engineering applications[1;2]. Porous, biodegradable scaffolds have been developed extensively in tissue engineering to regenerate musculoskeletal tissue[3-5]. Many combinations of materials and processing techniques have been used in order to attain the challenging requirements of an ideal tissue engineering scaffold.

One approach is to use a composite material. Composites have been applied to tissue engineering and particularly bone tissue engineering for 3 main reasons: a) Mechanical: the combination of the parent phases can modulate the mechanical properties of the scaffold, b) Chemical: the addition of one phase can minimize some drawbacks of the other, neutralising degradation products, for example, and c) Biological: one of the phases can enhance the biocompatibility or bioactivity or any other specific biological response of the whole[6]. In sum, the optimisation of the properties of a composite material should be more attainable and flexible than that of a single-phase material.

Combining a polymer and a ceramic material seems a sound approach for bone tissue engineering applications given that the structure of bone can be grossly described as a collagen-hydroxyapatite composite. Despite the well-documented biological properties of ceramics such as hydroxyapatite (HA), β-tricalcium phosphate (β-TCP) or bioactive glasses, their application in clinical cases is limited due to their mechanical characteristics. In fact, ceramics are very brittle and cannot withstand bending or torsion. Furthermore, their processing into complex or highly porous forms is not straightforward. Polymer-ceramic composites seek to combine the excellent bioactive properties of some ceramic materials with the processability and ease of manufacture of polymers.

Table 2.1 lists some recent studies combining polymers and ceramics to produce composite scaffolds. HA is usually introduced into the scaffolds in the shape of short

fibres or particles. Short fibres seem to reinforce the polymeric matrix to a greater extent than particles[7], although this effect is limited to low-porosity foams. HA reinforced scaffolds have very good bone-bonding abilities and in-vivo studies show no fibrous tissue capsule between the implant and the bone[8]. Bioglass® reinforced scaffolds form a surface layer of apatite which also enhances bone bonding capacities[9;10].

| **Polymeric matrix** | **Ceramic phase** | **Reference** |
|---|---|---|
| PLAGA | HA | [9] |
| PDLLA | Bioglass® | [11-14] |
| Chitosan | β-TCP | [15] |
| PLLA | Apatite layer formed in-situ | [8] |
| PDLLA | Wollanstonite | [16] |
| Polyhydroxybutyrate/polyhydroxyhexanoate | HA | [17] |
| PLGA | HA fibres | [7] |
| PLLA | HA | [18] |
| PDLLA | Calcium Phosphate soluble glass | [19;20] |

**Table 2.1:** Studies exploiting the composite approach to produce scaffolds for tissue engineering

There are two recurring challenges concerning polymer-ceramic scaffolds: mechanical properties and bioresorbability. Firstly, the mechanical properties of the scaffolds are often unsuitable for high load bearing applications such as bone substitution, or should be considered as a complement to other forms of stabilisation such as internal or external fixation. High porosity is virtually incompatible with high mechanical properties and thus a compromise must be attained without sacrificing pore interconnectivity. Secondly, both HA and Bioglass® have extremely low resorption rates. This implies the ceramic particles will remain within the newly formed bone long after it has remodelled, some authors believe this may cause a certain degree of stress-shielding[2]. Thus the application of β-TCP, with a much higher resorption rate, is also being pursued.

This chapter describes the development of composite scaffolds combining a polylactic acid polymer with a completely degradable calcium phosphate glass, by a solvent casting procedure. The influence of scaffold composition on the porosity and mechanical properties of the scaffolds has been measured and optimised by means of factorial experimental designs.

## *Materials and Methods*

## *Materials*

### PLA and calcium phosphate glass

The polymer used is a high molecular weight poly-95LL/5DL-lactic acid (PLA) from PURAC Biochem (Gorichem, The Netherlands). It is a copolymer of the LL and DL polylactic acids with 95% and 5% of each, respectively. Its molecular weight ($M_w$) was measured in a previous study at $3.33\times10^5$ by Gel Permeation Cromatography [20]. The material characteristics as given by the manufacturers are:

| | |
|---|---|
| Intrinsic viscosity | 6.6 dl/g |
| Fusion range | 163.4-172.4°C (DSC, 10°Cmin$^{-1}$) |
| Heat of fusion | 36.3 J/g (DSC, 10°Cmin$^{-1}$) |
| Residual solvent | < 0.1% |
| Residual monomer | <3% |

**Table 2.2:** Properties of the P-LL/DL-LA used in this study

The biodegradable glass used in this study is a titania-stabilised, completely degradable, calcium phosphate glass. For sake of simplicity, it will be called G5 glass from now on in the text, following the nomenclature used in previous publications. Its molar composition is:

| Molar composition | Compound |
|---|---|
| 44.5% | CaO |
| 44.5% | $P_2O_5$ |
| 6% | $Na_2O$ |
| 5% | $TiO_2$ |

**Table 2.3:** Molar composition of the titania-stabilised calcium phosphate glass used in the study

The G5 glass was elaborated following a three-step procedure[21;22]. All compounds were provided by Panreac Química S.A. First, $CaCO_3$ is calcinated at 900°C (Figure 2.1) in order to obtain CaO by reaction {1}:

$$CaCO_3 \xrightarrow{825^{\circ}C} CaO + CO_2 \qquad \{1\}$$

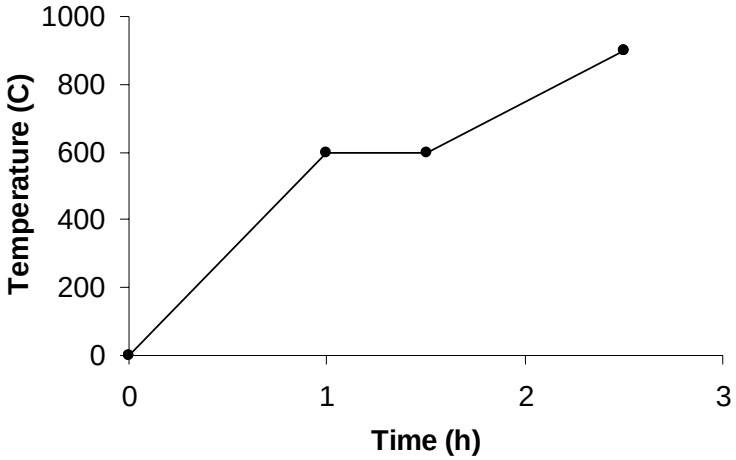


**Figure 2.1:** Temperature cycle for the calcination of $CaCo_3$

Next, the Ca0 is mixed with the other ingredients shown in Table 2.3, placed in a platinum crucible, and melted at 1350°C following the cycle illustrated in Figure 2.2. The mixture remains at 1350°C for eight hours in order to ensure complete homogeneity of the molten matter. After eight hours, the molten glass is quenched on a stainless steel plate heated at 480°C, and is annealed at 533°C (the glass transition temperature of the G5 glass) for 30 minutes. The glass cools to form transparent slabs, which are then

milled and sieved within a certain range. The properties of the G5 glass manufactured with this procedure can be seen in Table 2.4.

| | |
|---|---|
| Density | 2.903 $gcm^{-3}$ |
| Glass Transition Temperature | 532.9 °C |
| Rate of dissolution | $3.2\times10^{-7}$ $g/cm^2/h$ |
| Vickers Hardness | 431.1 $(kg/mm^2)$ |

**Table 2.4:** Properties of the G5 glass used in this study

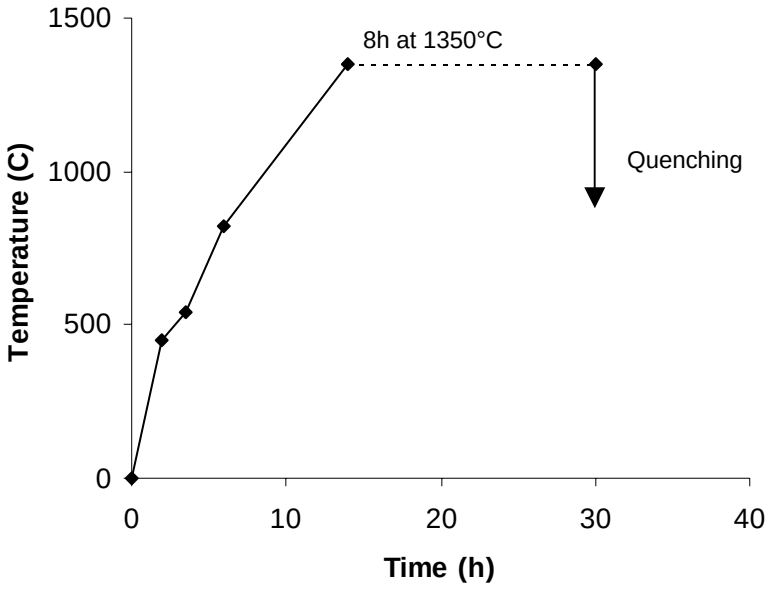


**Figure 2.2:** Temperature cycle of the fusion of the G5 glass

## *Methods*

### Factorial Experiment Design

In order to optimise certain mechanical and microstructural properties of the scaffolds, it is necessary to evaluate the influence of their composition and processing. This is a clear case in which factorial experiment design, in terms of compositional and processing factors, can help to optimise the properties of the material. A factorial experiment design is a statistical study in which each observation is categorised

according to more than one factor. The results can then be analysed by regression analysis in order to create a linear model which describes the behaviour of the system as a function of the factors. Such an experimental set-up and analysis allows studying the effect of each factor on the response, while requiring fewer observations than by conducting separate experiments for each factor independently. It also allows studying the effect of the interaction between factors on the response variable[23].

The response variable is the measurement or characteristic which is studied. The factors are the variables which have been included in the experiment because they are believed to influence the response. Finally, the factors are varied between different values or levels. In the case of this study, the response is the porosity or mechanical properties of the scaffolds, the factors are ingredients of the composition such as the amount of glass and the levels are the percents of glass, 20% or 50% for example.

Factorial experiment designs in which each factor varies between two levels are most commonly used in research and industrial applications. In this case, the values of the factors corresponding to each level are parameterised into a low level and a high level, or -1 and +1 respectively. Two-level factorial designs optimise the results obtained with respect to the experimental effort, they are simple to design, perform and analyse, and can be easily combined to obtain a larger experiment. Two-level factorial designs can be abbreviated as $2^k$ where k stands for the number of factors used.

The first step in a factorial experiment design is to specify the problem and determine which responses (Y) and factors (X) will be evaluated. The levels of the factors must then be chosen as an educated guess, given that the analysis assumes the response varies linearly between the two levels. The experimental runs must be randomised in order to avoid or reduce the influence of uncontrollable factors on the output. Finally, the responses are analysed and a saturated linear model relating the factors and the response can be proposed:

$$Y = \phi(x) + \varepsilon \qquad \{2\}$$

Where Y is the response, $\phi(x)$ is a polynomial function of the factors, and ε is the error. If there were two factors, the saturated polynomial function $\phi$(x) would be:

$$\phi(x) = \beta_0 + \beta_1 X_1 + \beta_2 X_2 + \beta_{12} X_1 X_2, \qquad \{3\}$$

In this case, $\beta_1$ and $\beta_2$ are the effects of each factor and $\beta_{12}$ is the effect of the interaction of the factors. It is important to point out that the error should be independent of the factors.

In the case of saturated $2^k$ linear models, the significance of the effects cannot be calculated using the standard statistical methods (ANOVA regression). Instead the significance of the effects is calculated by comparing the distribution of the effects to a normal probability plot: the effects whose values do not follow a normal distribution are significant. In order to apply this method, the model must be saturated and the variances of the effects must be equal.

A $2^4$ factorial experiment design was applied in this study in order to evaluate the influence of the composition of the scaffolds on their porosity and mechanical properties. The factors and effects used in the study are described in detail below.

## Solvent Casting Procedure

A preliminary study on the development of solvent cast composite PLA/G5 scaffolds was performed by Navarro et al. [19]. The research described in this chapter involves the optimisation of the scaffold composition, manufacturing procedure and properties.

The composite scaffolds are manufactured by means of a solvent-casting salt-leaching method. First, PLA pellets are dissolved in chloroform at a 5% weight versus volume (w/v) ratio. The dissolution takes approximately two days on an orbital shaker at room temperature. Once the PLA is completely dissolved, sieved sodium chloride (NaCl) and glass particles are added to the mixture and mixed thoroughly, forming a thick paste. The paste is spread on a Teflon sheet or into moulds until complete chloroform evaporation. Samples are punched out of the dry paste, or unmoulded, and placed in distilled water for 48 hours in order to leach the NaCl out. After this time the samples are left to dry at room temperature. The NaCl particles leave behind a porous network.

### *$2^4$ factorial experiment design*

The characterisation and optimisation of the scaffolds was done by means of a four-factor factorial experiment design. The influence of four aspects of the composition; the four factors, on the morphology, porosity and mechanical properties of

the scaffolds was studied. The four factors were: a) weight percent (wt%) of NaCl, b) size of NaCl particles, c) size of G5 glass particles, and d) wt% of G5 glass particles. Each factor was tested at two levels: a maximum (+1) and a minimum (-1) (see Table 2.5), fabricating a total of 16 different compositions (see Table 2.6).

| | NaCl wt% | NaCl particle size (μm) | Glass particle size (μm) | Glass wt% |
|---|---|---|---|---|
| Low level (-1) | 75% | 80-210 | <40 | 20% |
| High level (+1) | 94% | 297-590 | 40-80 | 50% |

**Table 2.5:** Levels of the factors used for the $2^4$ experimental design

| Composition Nº | NaCl wt% | NaCl particle size | Glass particle size | Glass wt% |
|---|---|---|---|---|
| 1 | -1 | -1 | -1 | +1 |
| 2 | +1 | -1 | -1 | +1 |
| 3 | -1 | +1 | -1 | +1 |
| 4 | +1 | +1 | -1 | +1 |
| 5 | -1 | -1 | +1 | +1 |
| 6 | +1 | -1 | +1 | +1 |
| 7 | -1 | +1 | +1 | +1 |
| 8 | +1 | +1 | +1 | +1 |
| 9 | -1 | -1 | -1 | -1 |
| 10 | +1 | -1 | -1 | -1 |
| 11 | -1 | +1 | -1 | -1 |
| 12 | +1 | +1 | -1 | -1 |
| 13 | -1 | -1 | +1 | -1 |
| 14 | +1 | -1 | +1 | -1 |
| 15 | -1 | +1 | +1 | -1 |
| 16 | +1 | +1 | +1 | -1 |

**Table 2.6:** Composition of the 16 samples used for the characterisation

*Morphology*

A qualitative study of the scaffold morphology was performed by Scanning Electron Microscopy (SEM) on a Jeol JSM-6400.

*Porosity*

The porosity of the scaffolds was measured by mercury pycnometry. The apparent density of the scaffold ($\rho_{scaffold}$) was measured by means of the volume of mercury it displaced when submerged. The porosity of the scaffold is calculated by dividing its apparent density by the density of the solid composite ($\rho_{solid}$):

$$\%Porosity = 100\left(1 - \frac{\rho_{scaffold}}{\rho_{solid}}\right) \qquad \{4\}$$

The density of the solid composite, $\rho_{solid}$, is calculated using the densities of each phase: PLA = 1.231 $gcm^{-3}$ and G5 glass= 2.903 $gcm^{-3}$ (Table 2.4), as:

$$\frac{1}{\rho_{solid}} = \frac{wt\%_{PLA}}{\rho_{PLA}} + \frac{wt\%G5}{\rho_{G5}} \qquad \{5\}$$

Measurements are presented as an average of five samples.

*Compression tests*

Compression tests were performed on an Adamel Lhomargy universal testing machine, with a 100N load cell at a constant cross-head speed of 2mm/min until 50% strain of the sample or a maximum of 70N compressive stress. All compression samples had a diameter of 12mm. The height of the samples was approximately 10mm. The sample dimensions were chosen in order to avoid buckling, and reduce the effect of friction hills[24-27]. The stiffness of the scaffolds is defined as the slope of the initial linear portion of the stress strain curve, the slope was measured at intervals of 0.025 strain ($\varepsilon$) until the difference between the values was more than 10%, starting at $\varepsilon$ = 7.5%. Measurements are presented as an average of five samples.

## *Results and Discussion*

*Morphology*

The solvent casting method creates highly porous scaffolds as can be seen by SEM images. The effect of scaffold composition can be clearly seen in Figure 2.3. High NaCl wt% (even-numbered compositions) produce higher porosity and thinner pore walls. NaCl particle size visibly affects pore size. The glass particles are visible at higher magnifications, and their dimensions can be clearly seen in Figure 2.4. SEM images also reveal the morphology of the pore walls, which is indicative of the interconnectivity of the porosity. Compositions with low NaCl wt% present very compact pore walls whereas highly porous scaffolds have thin porous pore walls. The

wt% of NaCl particles also influences the coating of the glass particles within the polymer matrix: at high NaCl wt%, the glass particles sit loosely within the PLA matrix whereas at low NaCl wt% they are embedded within the pore wall (Figure 2.5).

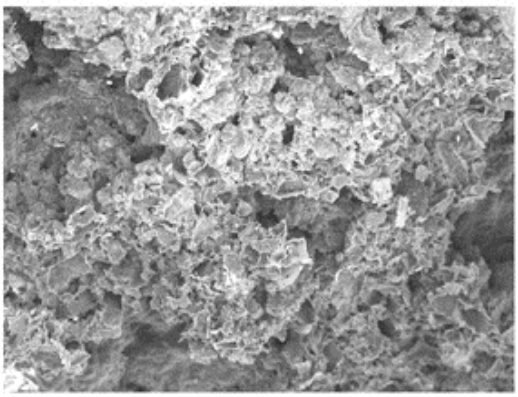
1

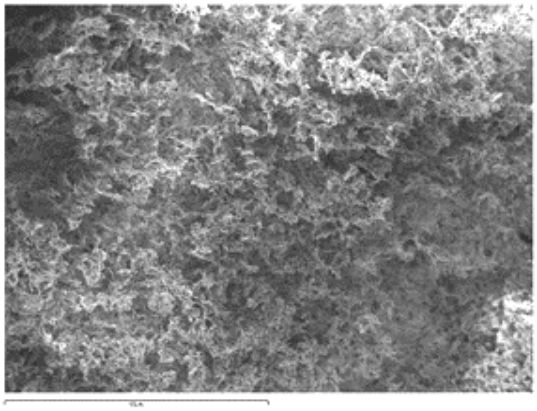
2

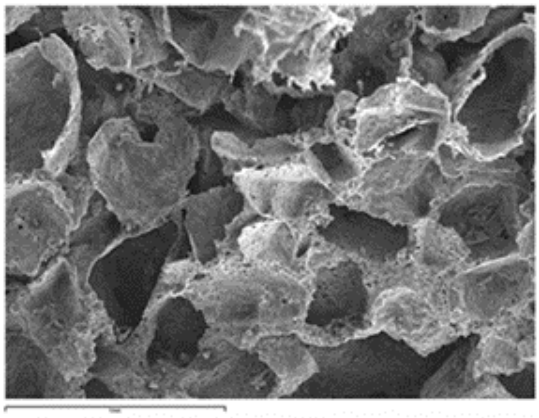
3

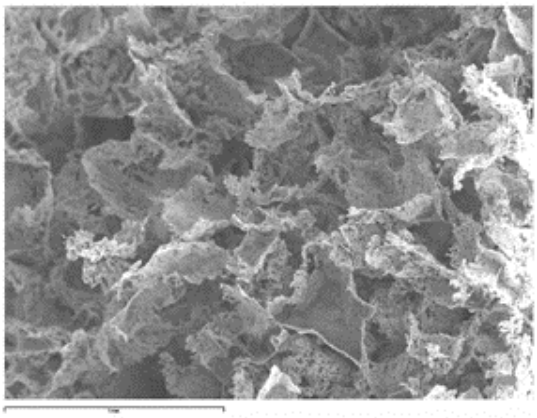
4

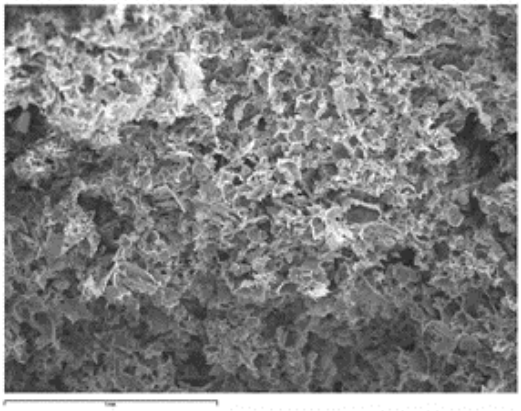
5

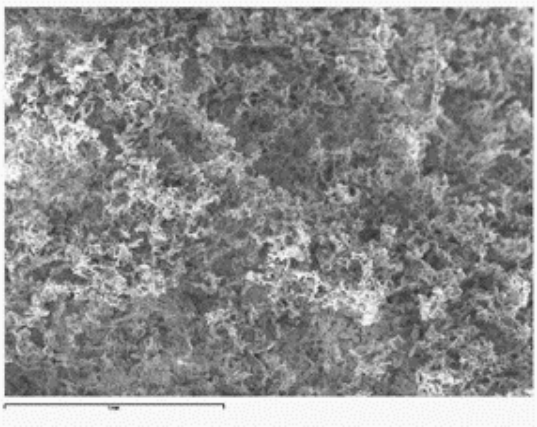
6

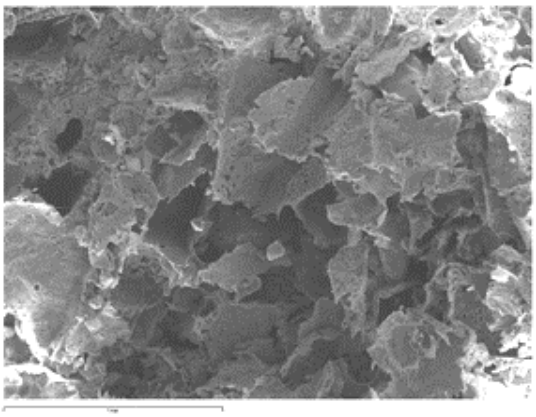
7

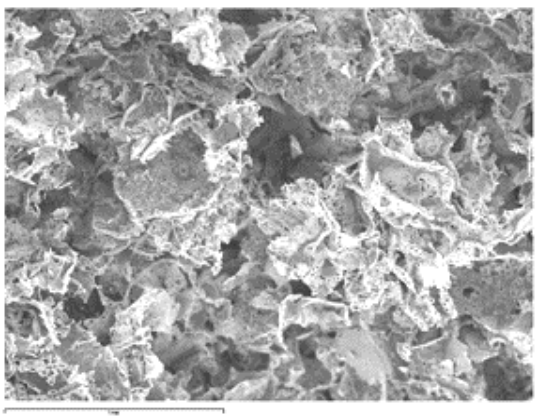
8

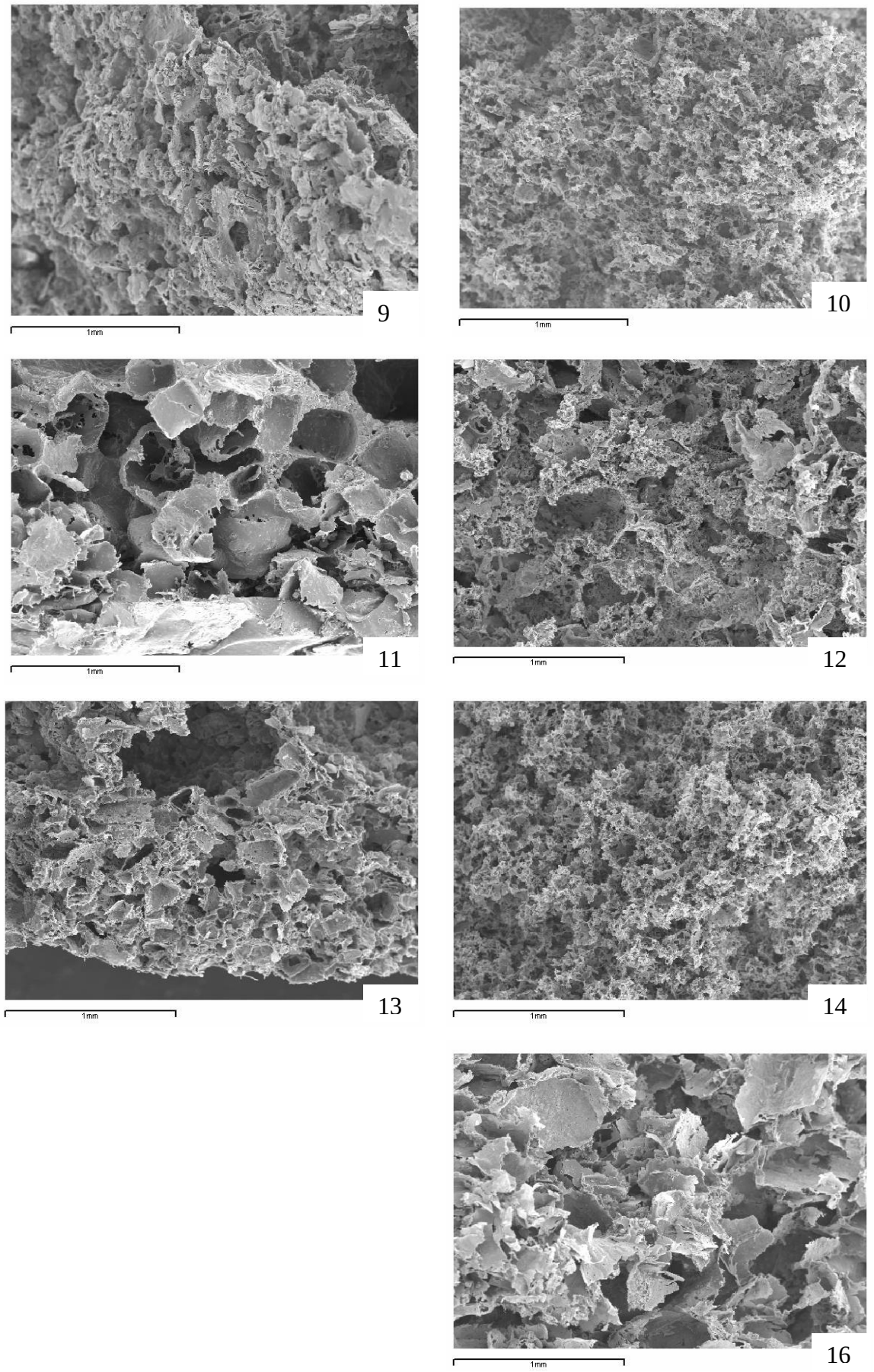


**Figure 2.3:** SEM images of compositions 1-16 of the experimental design. All magnification bars correspond to 1mm. (Image for composition nº 15 is missing due to technical problems).

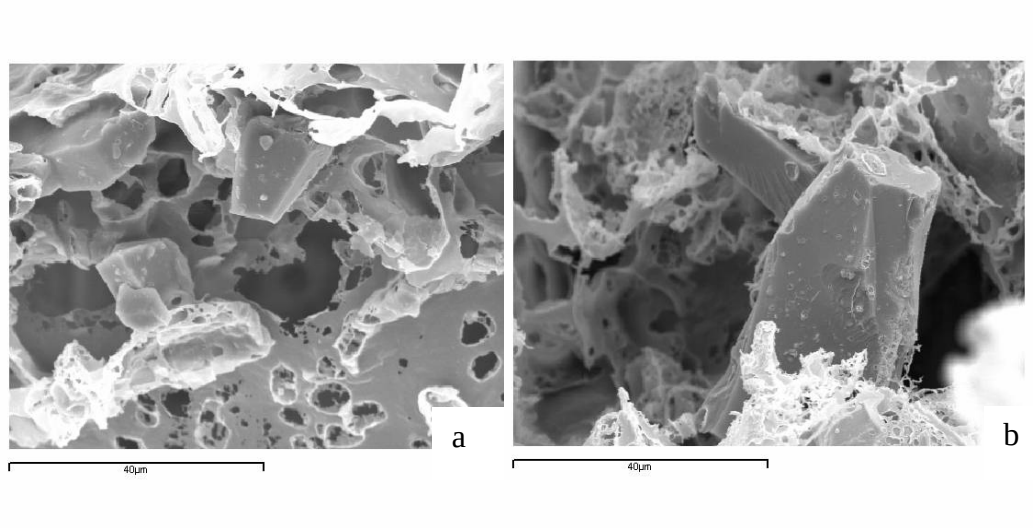


**Figure 2.4:** SEM images of a) glass particles sieved to <40mm in composition nº 12 and b) glass particles sieves between 40 and 80mm in composition nº14. All magnification bars correspond to 40µm.

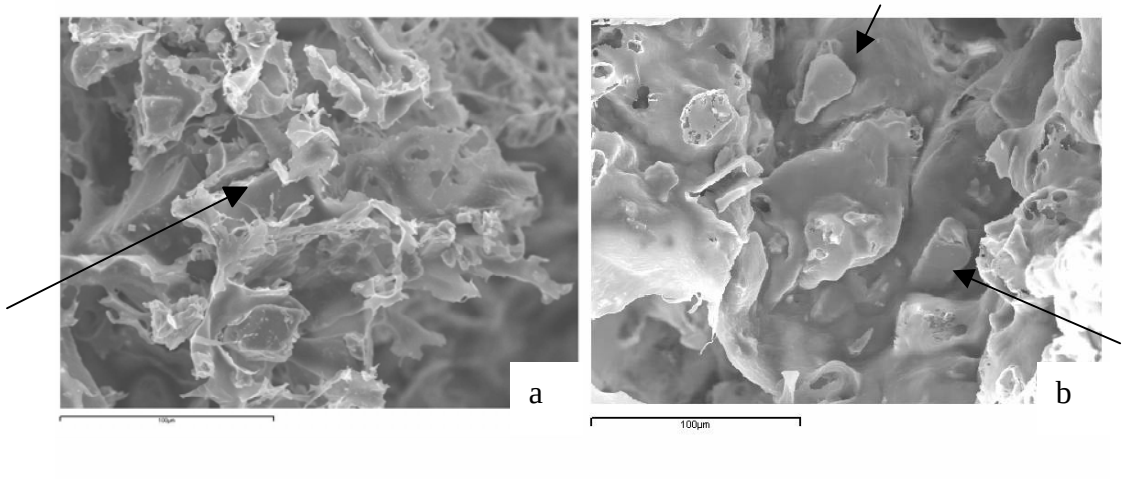


**Figure 2.5:** SEM images revealing the morphology of the pore walls and the coating of the glass particles by the polymer, in a) composition nº2 with highly porous pore walls and poorly coated glass particles (see arrow), and b) composition nº9 with compact pore walls and well coated glass particles. All magnification bars correspond to 100µm.

*Porosity*

The porosity results for composition 1-16 can be seen in Figure 2.6. (The numerical values can be seen in the Appendix Chapter 2). The porosity ranges between 66% and 96%. Even-numbered compositions, with 94 wt% of NaCl particles, have higher porosities than odd-numbered compositions.

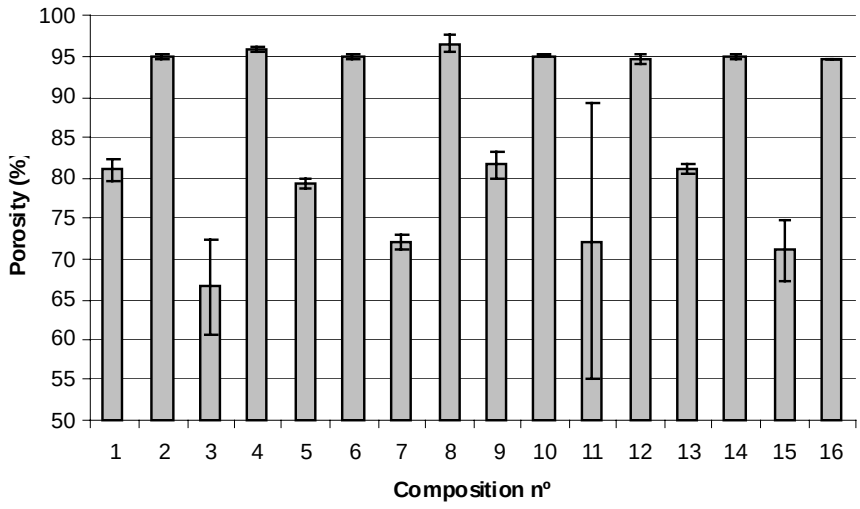


**Figure 2.6:** Porosity results for compositions 1-16.

*Compression tests*

The compression test results for composition 1-16 can be seen in Figure 2.7. (The numerical values can be seen in the Appendix Chapter 2). The stiffness ranges between 100 and 600 kPa. Even-numbered compositions, with 94 wt% of NaCl particles, have lower stiffness and higher porosities, than odd-numbered compositions.

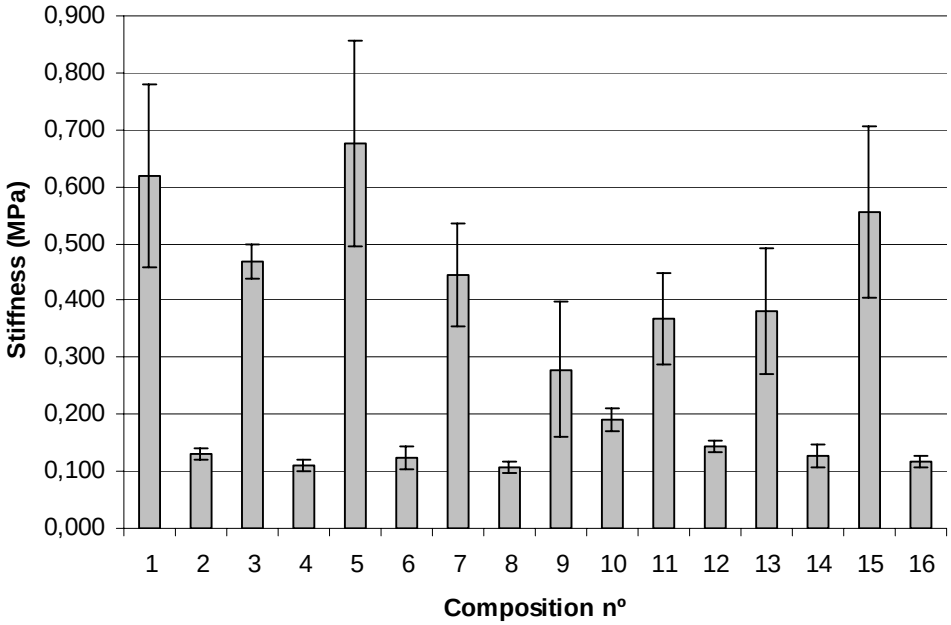


**Figure 2.7:** Stiffness results for compositions 1-16

*Experiment Design Analysis*

The porosity and compression results for compositions nº 1-16 were analysed using factorial experiment design analysis. For the sake of simplicity, the detailed calculations of the factorial experiment design can be seen in Appendix Chapter 2. The polynomial parameters have been adjusted according to the model described in the Methods/ Factorial Experiment Design, paragraph nº 4.

Three factors were found to have a significant effect on the porosity readings: the NaCl wt%, NaCl particle size, and the interaction between the two. The linear model would read as follows:

$$\textbf{\textit{Porosity}}\ \textbf{(\%)} = 85.4 + 9.8\times\Delta NaCl + 2.7\times\Delta NaCl\times\phi NaCl - 2.5\times\phi NaCl \qquad \{6\}$$

where ΔNaCl stands for NaCl wt%, ϕNaCl stands for NaCl particle size, and the values of NaCl wt% and particle size correspond to the levels shown in Table 2.5.

Thus, the porosity of the scaffolds within this range of factors depends only on the amount and size of the porogen (NaCl), not on the glass particles. The most important effect is that of the NaCl wt%, which is positive; higher wt% of NaCl increase the porosity of the scaffolds (Figure 2.8). The NaCl particle size also influences the porosity significantly; higher NaCl particle sizes decrease the porosity of the scaffold, this effect is, however, not as pronounced as the former (Figure 2.9).

The effect of the interaction between the NaCl particle size and wt% can be seen in Figure 2.10; at high NaCl wt% the NaCl particle size has practically no effect on the porosity whereas it decreases porosity at low NaCl wt%.

The results are logical since the NaCl is the porogen agent, and thus it should be expected to increase the porosity of the scaffolds. The fact that the glass phase does not affect the porosity significantly is interesting because it would allow the scaffolds to contain high glass wt% without compromising their porosity.

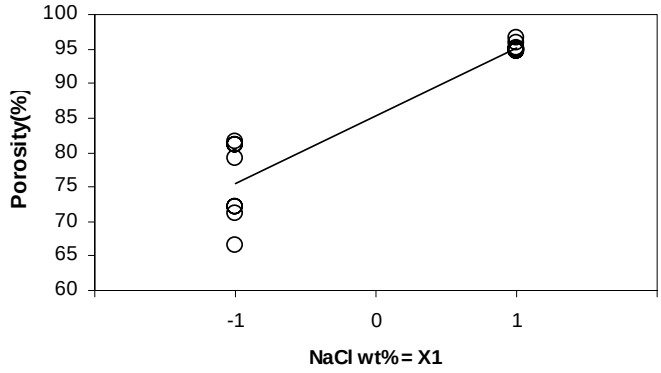


**Figure 2.8:** Effect of the NaCl wt% (X1) on the porosity of the scaffolds. The line indicates the tendency of the average value of the porosity as the value of NaCl wt% (X1) varies from –1 to +1.

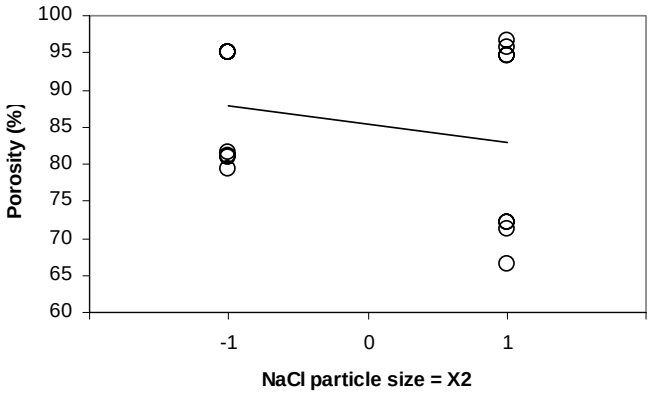


**Figure 2.9:** Effect of NaCl particle size (X2) on the porosity of the scaffolds. The line indicates the tendency of the average value of the porosity as the value of NaCl particle size (X2) varies from –1 to +1.

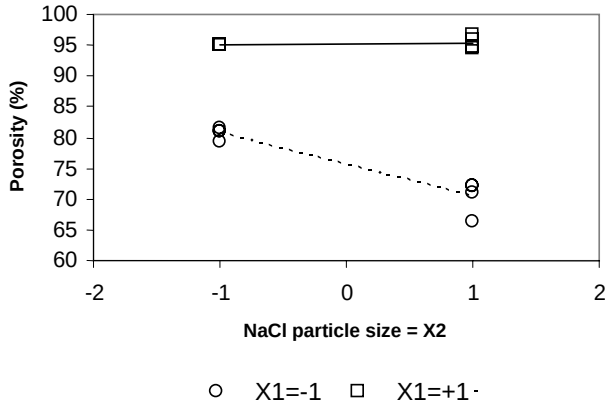


**Figure 2.10:** Effect of the interaction between NaCl wt% (X1) and NaCl particle size (X2) on the porosity of the scaffolds. The dotted line indicates the tendency of the average value of the porosity as NaCl particle size (X2) varies from –1 to +1 when the NaCl wt% (X1) is -1. The full line indicates the tendency of the average value of the porosity as the value of NaCl particle size (X2) varies from –1 to +1 when the NaCl wt% (X1) is +1.

In the case of the stiffness readings, it is clear in Figure 2.7, that the standard deviations of the odd-numbered compositions are larger than those of the even-numbered compositions. This implies that the NaCl wt% not only affects the stiffness of the scaffolds, but also the variability of the result. Thus, the results cannot be interpreted by applying a saturated linear model. Effectively, 75wt% of NaCl particles made the scaffold structure more heterogeneous (Figure 2.3).

In order to analyse the effects of the remaining factors on scaffold stiffness, the low level of the NaCl wt% was eliminated from the experiment design leaving a $2^3$ design with the following factors: NaCl particle size, glass particle size and glass wt% (only the even-numbered compositions from Table 2.1). For the sake of simplicity, the detailed calculations of the factorial experiment design can be seen in Appendix Chapter 2. The polynomial parameters have been adjusted according to the model described in the Methods/ Factorial Experiment Design, paragraph nº 4.

In this $2^3$ experimental design, three factors and one interaction were found to have a significant effect on the stiffness: the glass wt%, the glass particle size, the NaCl particle size and the interaction between the glass wt% and particle size. The linear model would read as follows:

$$\textbf{\textit{Stiff.}} = 0{,}131 - 0{,}013 \times \Delta Glass - 0{,}0125 \times \phi Glass - 0{,}0120 \times \phi NaCl + 0{,}010 \times \Delta Glass \times \phi Glass \quad \{7\}$$

where ΔGlass stands for Glass wt%, ϕGlass stands for Glass particle size, ϕ NaCl stands for NaCl particle size, and the values of all factors correspond to the levels shown in Table 2.5. The value of the stiffness would be in MPa.

All factors have a significant negative effect on scaffold stiffness. An increase in the amount and size of the glass particles or in the size of the NaCl particles decreases the stiffness of the scaffolds (Figure 2.11, 2.13 and 2.14). Furthermore, there is an interaction between the glass particle size and the glass wt%. At high glass wt% the effect of the glass particle size is much smaller than at low glass wt% (Figure 2.14). Thus, both the pores and the glass particles act as defects in the porous PLA matrix.

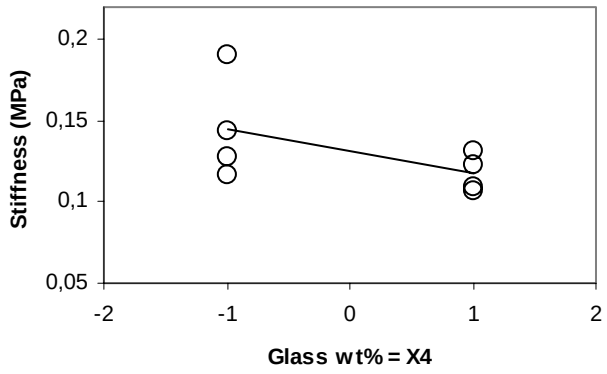


**Figure 2.11:** Effect of the glass wt% (X4) on the stiffness of the scaffolds. The line indicates the tendency of the average value of the stiffness as the value of the glass wt% (X4) varies from –1 to +1.

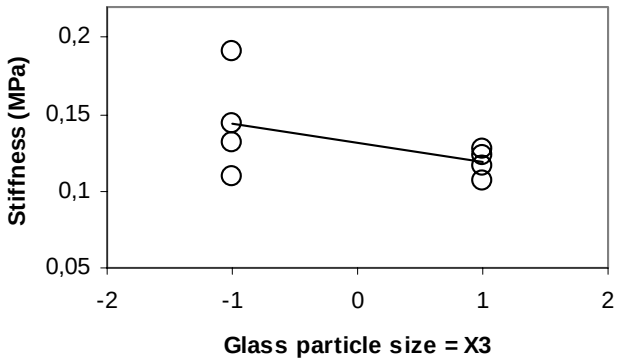


**Figure 2.12:** Effect of the glass particle size (X3) on the stiffness of the scaffolds. The line indicates the tendency of the average value of the stiffness as the value of the glass particle size (X3) varies from –1 to +1.

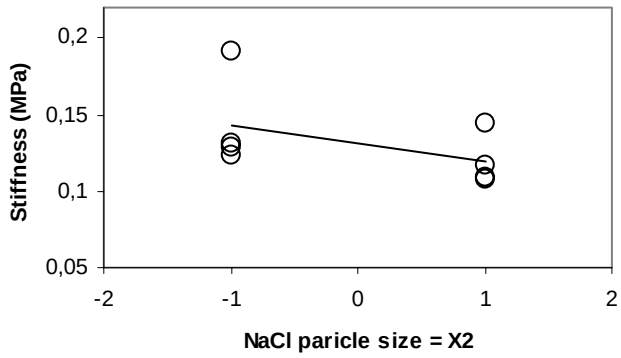


**Figure 2.13:** Effect of the NaCl particle size (X2) on the stiffness of the scaffolds. The line indicates the tendency of the average value of the stiffness as the value of the NaCl particle size (X2) varies from –1 to +1.

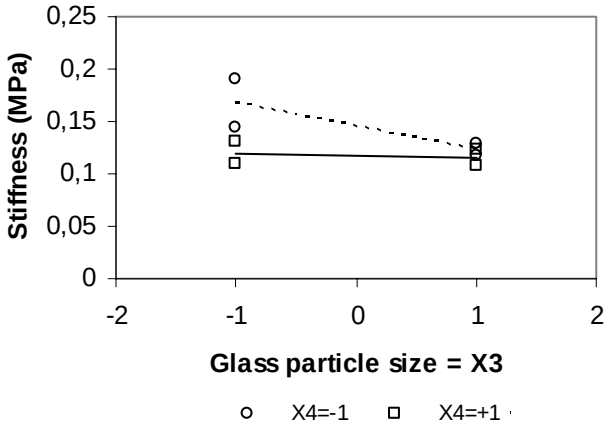


**Figure 2.14:** Effect of the interaction between the glass particle size (X3) and the glass wt% (X4). The dotted line indicates the tendency of the average value of the stiffness as the glass particle size (X3) varies between –1 to +1 when the glass wt% (X4) is -1. The full line indicates the tendency of the average value of the stiffness as the value of the glass particle size (X3) varies from –1 to +1 when the glass wt% (X4) is +1 .

The experiment design reveals that the scaffolds' mechanical properties can be modulated by adjusting their composition without compromising their porosity. Indeed, a theoretical calculation of the volume fraction occupied by the composite in the scaffolds (see detailed calculations in Appendix Chapter 2), gives a porosity of 90.7% at 20wt% of glass particles, and 92.5% at 50wt% of glass particles at high NaCl wt%. Thus a difference of only 1.8% porosity between the two levels of glass wt%. This

small difference is probably effaced by experimental error during scaffold processing and porosity measurements.

Increasing the NaCl particle size decreases the porosity of the scaffolds (Figure 2.9). This could be due to a less efficient packing of the large NaCl particles. The interaction between the NaCl particle size and NaCl wt% (Figure 2.10) could be due to the fact that at 94 wt% the PLA-glass paste is saturated with NaCl particles and has attained its maximum porosity. Thus no further changes in the nature or quantity of the NaCl particles affect the overall porosity. Indeed, the change of NaCl particle size should then alter the nature of the porosity: pore size, pore interconnectivity and pore wall size, but not the total porosity.

Increasing the glass wt% and the NaCl particle size decreases the stiffness of the scaffold. Thus, both the pores and the glass particles seem to act as defects which undermine the scaffolds' stiffness. These results conform with Thomson et al.[28] and Wang et al.[29] results. Both authors find that Young's Modulus and yield stress of high porosity scaffolds decrease with an increase of filler content. This is because at high porosities, pore walls are too thin to be able to fasten and interact with the filler particles, thus they act a defects in the matrix. The values of the stiffness of the scaffolds correspond to those reported by other authors with similar porosities and compositions [29-33].

Concerning the NaCl particle size, as mentioned above, the larger the NaCl particle, the lower the stiffness of the scaffold. A theoretical calculation of the thickness of the pore walls (see details in Appendix Chapter 2) as a function of scaffold composition reveals that pore walls are thicker at large NaCl particle sizes (Table 2. 7). This does not mean the scaffolds will be stiffer however, since the pores are much larger in the case of large NaCl particles. At 50wt% of glass, the difference between the pore wall thickness at both NaCl particle size levels, is smaller than at 20wt% of glass.

All interpretations of the results that take into account NaCl particle packing and average sizes must be interpreted with caution however, since the NaCl particles were not characterised prior to mixing, thus thie rrange of sizes and shapes is unkown.

| NaClwt% | Glas wt% | NaCl particle size | Pore wall thickness |
|---|---|---|---|
| 94% | 20% | [80-210]μm | 1.5 μm |
| 94% | 20% | [297-590]μm | 8 μm |
| 94% | 50% | [80-210]μm | 3.5 μm |
| 94% | 50% | [297-590]μm | 7 μm |

**Table 2. 7:** Theoretical calculation of pore wall thickness as a function of scaffold composition

The information from the experiment design can be used to choose the optimum scaffold composition. Regarding porosity, all composition with a NaCl wt% of 94% would give an adequate porosity. In fact all high NaCl wt% compositions have porosities around 95%.

Regarding stiffness, the results indicate that the size of NaCl and glass particles should be reduced in order to increase the stiffness of the scaffolds. Ideally, the glass wt% should also be reduced, although the potential biological benefits of 50wt% of glass would probably outweigh its detrimental effect on scaffold mechanical properties. Taking these criteria into account, compositions nº 2 and nº 10 were chosen to pursue further characterisations and experiments during this thesis (Table 2.8).

| Composition nº | NaCl wt% | NaCl particle size (μm) | Glass particle size (μm) | Glass wt% |
|---|---|---|---|---|
| 2 | 94% | 80-210 | <40 | 20% |
| 10 | 94% | 80-210 | <40 | 50% |

**Table 2.8:** Detailed compositions of scaffolds with composition nº 2 and nº 10, with an optimal combination of porosity and stiffness

## *Conclusions*

- SEM images prove that the NaCl wt% and NaCl particle size affect scaffold pore morphology. NaCl wt% determines the overall porosity, and NaCl particle size determines the size of the pores
- SEM images reveal glass particles that sit loosely within the PLA matrix

This could be due to the fact that at 94 wt% the PLA-glass paste is saturated with NaCl particles and has attained its maximum porosity. Thus no further changes in the nature or quantity of the NaCl particles affect the overall porosity. Indeed, the change of NaCl particle size should then alter the nature of the porosity: pore size, pore interconnectivity and pore wall size, but not the total porosity.

- A NaCl wt% of 75% was inadequate for this processing method, it created heterogeneous morphologies and affected the variability of the stiffness readings
- The experiment design revealed that the porosity depended on the NaCl wt%, the NaCl particle size and the interaction between the two (Table 2.9).
- The experiment design analysis revealed that the stiffness depended on the glass wt% and particle size and their interaction, and on the NaCl particle size.

| | NaCl wt% | NaCl particle size | Glass particle size | Glass wt% |
|---|---|---|---|---|
| Porosity | ↑ * | ↓ * | / | / |
| Stiffness | Not applicable | ↓ | ↓* | ↓* |

**Table 2.9** Factors of scaffold composition that had a significant effect on the porosity and stiffness of the scaffolds. ↑ stands for a positive effect, ↓ stands for a negative effect, and * stands for an interaction.

- Compositions nº 2 and nº 10 have been chosen to continue characterisation and experimentation. Their composition can be seen in Table 2.8.

## Publications

The results of this study have been published in:

"Development of biodegradable composite scaffolds for bone tissue engineering: physicochemical, topographical, mechanical, degradation and biological properties"
M.Navarro, C. Aparicio, M.Charles-Harris, E.Engel, M.P.Ginebra, J.A.Planell
Advances in Polymer Science 2006; vol 200, pp 209-215

"Mechanical and structural characerisation of completely degradable polylactic acid/calcium phosphate glass scaffolds"
M.Charles-Harris, S. del Valle, E.Hentges, P.Bleuet, D.Lacroix, J.A.Planell
Biomaterials 2007, vol 28, pp 4429-4438

## *Bibliography*


(1) Widmer MS, Mikos AG. Fabrication of Biodegradable Polymer Scaffolds. In: Patrick CW, Mikos AG, Mc.Intre L, editors. Frontiers in Tissue Engineering. Oxford: Elsevier Science Ltd., 1998: 107-120.

(2) Yaszemski MJ, Payne RG, Hayes WC, Langer R, Mikos AG. Evolution of bone transplantation: molecular, cellular and tissue strategies to engineering human bone. Biomaterials 1996; 17:175-185.

(3) Hutmacher DW. Scaffolds in tissue engineering bone and cartilage. Biomaterials 2000; 21:2529-2543.

(4) Bonassar LJ, Vacanti CA. Tissue engineering: the first decade and beyond. J Cell Biochem Suppl 1998; 30-31:297-303.

(5) Langer R, Vacanti JP. Tissue engineering. Science 1993; 260(5110):920-926.

(6) Laurencin CT, Lu HH. Polymer-Ceramic Composites for Bone-Tissue Engineering. In: Davies JE, editor. Bone Engineering. Toronto: em squared, 2000: 462-472.

(7) Thomson RC, Yaszemski MJ, Powers JM, Mikos AG. Hydroxyapatite fiber reinforced poly(α-hydroxy ester) foams for bone regeneration. Biomaterials 1998; 19:1935-1943.

(8) Zhang R, Ma PX. Porous poly(L-lactic acid)/apatite composites created by biomimetic process. J Biomed Mater Res 1999; 45(4):285-293.

(9) Devin JE, Attawia MA, Laurencin CT. Three-dimensional degradable porous polymer-ceramic matrices for use in bone repair. J Biomater Sci Polym Ed 1996; 7(8):661-669.

(10) Marcolongo M, Ducheyne P, Garino J, Schepers E. Bioactive glass fiber/polymeric composites bond to bone tissue. J Biomed Mater Res 1998; 39(1):161-170.

(11) Maquet V, Boccaccini AR, Pravata L, Notingher I, Jerome R. Preparation, characterization, and in vitro degradation of bioresorbable and bioactive composites based on Bioglass-filled polylactide foams. J Biomed Mater Res A 2003; 66(2):335-346.

(12) Boccaccini AR, Notingher I, Maquet V, Jerome R. Bioresorbable and bioactive composite materials based on polylactide foams filled with and coated by Bioglass particles for tissue engineering application. Journal of Materials Science: Materials in Medicine 2003; 14:443-450.

(13) Maquet V, Boccaccini AR, Pravata L, Notingher I, Jerome R. Porous poly(alpha-hydroxyacid)/Bioglass composite scaffolds for bone tissue

engineering. I: Preparation and in vitro characterisation. Biomaterials 2004; 25(18):4185-4194.

(14) Roether JA, Gough JE, Boccaccini AR, Hench LL, Maquet V, Jerome R. Novel bioresorbable and bioactive composites based on bioactive glass and polylactide foams for bone tissue engineering. J Mater Sci Mater Med 2002; 13(12):1207-1214.

(15) Zhang Y, Zhang M. Synthesis and characterization of macroporous chitosan/calcium phosphate composite scaffolds for tissue engineering. J Biomed Mater Res 2001; 55:304-312.

(16) Li H, Chang J. Preparation and characterization of bioactive and biodegradable Wollastonite/poly(D,L-lactic acid) composite scaffolds. J Mater Sci Mater Med 2004; 15(10):1089-1095.

(17) Wang YW, Wu Q, Chen J, Chen GQ. Evaluation of three-dimensional scaffolds made of blends of hydroxyapatite and poly(3-hydroxybutyrate-co-3-hydroxyhexanoate) for bone reconstruction. Biomaterials 2005; 26(8):899-904.

(18) Gross KA, Rodriguez-Lorenzo LM. Biodegradable composite scaffolds with an interconnected spherical network for bone tissue engineering. Biomaterials 2004; 25(20):4955-4962.

(19) Navarro M, Ginebra MP, Planell JA, Zeppetelli S, Ambrosio L. Development and cell response of a new biodegradable composite scaffold for guided bone regeneration. J Mater Sci Mater Med 2004; 15(4):419-422.

(20) Navarro M, Aparicio C, Charles-Harris M, Ginebra MP, Engel E, Planell JA. Development of a biodegradable composite scaffold for bone tissue engineering: physico-chemical, topographical, mechanical, degradation and biological properties. Advances in Polymer Science 2006; 200:209-231.

(21) Clément J. Desarrollo y caracterización de un material compuesto totalmente biodegradable para aplicaciones quirúrgicas. Universitat Politècnica de Catalunya, 2001.

(22) Navarro M, Ginebra MP, Clement J, Martinez S, Avila G, Planell JA. Physicochemical degradation of titania-stabilized soluble phosphate glasses for medical applications. Journal of the American Ceramic Society 2003; 86(8):1345-1352.

(23) Pepió M, Polo C. Diseño de experimentos y optimización de procesos. Terrassa: LESTAD ETSEIT UPC, 2003.

(24) Dieter GE. Mechanical Metallurgy. Second Edition, International Student Edition ed. Mc Graw-Hill International Book Company, 1981.